

# Stability of Highly Hydrogenated Monolayer Graphene in Ultra-High Vacuum and in Air

Alice Apponi<sup>\*1,2</sup>, Orlando Castellano<sup>1,2</sup>, Daniele Paoloni<sup>1,2</sup>, Domenica Convertino<sup>3</sup>, Neeraj Mishra<sup>3</sup>, Camilla Coletti<sup>3,4</sup>, Andrea Casale<sup>5</sup>, Luca Cecchini<sup>8</sup>, Alfredo G. Cocco<sup>6</sup>, Benedetta Corcione<sup>7,8</sup>, Nicola D'Ambrosio<sup>6</sup>, Angelo Esposito<sup>7,8</sup>, Marcello Messina<sup>6</sup>, Francesco Pandolfi<sup>8</sup>, Francesca Pofi<sup>6,9</sup>, Ilaria Rago<sup>8</sup>, Nicola Rossi<sup>6</sup>, Sammar Tayyab<sup>7,8</sup>, Ravi Prakash Yadav<sup>7,8</sup>, Federico Virzi<sup>6,10</sup>, Carlo Mariani<sup>7,8</sup>, Gianluca Cavoto<sup>7,8</sup>, and Alessandro Ruocco<sup>1,2</sup>

<sup>1</sup>*Dipartimento di Scienze, Università degli Studi di Roma Tre,*

*Via della Vasca Navale 84, 00146 Roma, Italy*

<sup>2</sup>*INFN Sezione di Roma Tre, Via della Vasca Navale 84, 00146 Roma, Italy*

<sup>3</sup>*Center for Nanotechnology Innovation @NEST,*

*Istituto Italiano di Tecnologia, Pisa, Italy*

<sup>4</sup>*Graphene Labs, Istituto italiano di tecnologia,*

*Via Morego 30, I-16163 Genova, Italy*

<sup>5</sup>*Department of Physics, Columbia University,*

*538 West 120th Street, New York, New York 10027, USA*

<sup>6</sup>*INFN-LNGS, Via G. Acitelli 22,*

*67100 Assergi-L'Aquila, L'Aquila, Italy*

<sup>7</sup>*Sapienza Università di Roma, Piazzale Aldo Moro 2, 00185 Roma, Italy*

<sup>8</sup>*INFN Sezione di Roma, Piazzale Aldo Moro 2, 00185 Roma, Italy*

<sup>9</sup>*Gran Sasso Science Institute, Viale Francesco Crispi 7, 67100 L'Aquila, Italy and*

<sup>10</sup>*Università degli Studi dell'Aquila,*

*Piazza Santa Margherita 2, 67100 L'Aquila, Italy*

---

\* Corresponding author. E-mail: alice.apponi@roma3.infn.it

## Abstract

The stability of hydrogenated monolayer graphene was investigated via X-ray photoemission spectroscopy (XPS) for two different environmental conditions: ultra-high vacuum (UHV) and ambient pressure. The study is carried out by measuring the C 1s line shape evolution for two hydrogenated samples one kept in the UHV chamber and the other progressively exposed to air. In particular, the  $sp^3$  relative intensity in the C 1s core-level spectrum, represented by the area ratio  $\frac{sp^3}{sp^2+sp^3}$ , was used as a marker for the hydrogenation-level and it resulted to vary by  $(4 \pm 2)\%$  in UHV after four months. Thus, a long-term stability of hydrogenated monolayer graphene was found, that indicates this material as a good candidate for hydrogen (or tritium) storage as long as it is kept in vacuum. On the other hand, the C 1s spectrum of the sample exposed to air shows a significant oxidation. A rapid growth up to saturation of the carbon oxides was observed with a time constant  $\tau = 1.8 \pm 0.2$  hours. Finally, the re-exposure of the oxidised sample to atomic hydrogen was found to be an effective method for the recovery of hydrogenated graphene. This process was studied by carrying out both XPS and electron energy loss spectroscopy, the latter exploited to observe the CH stretching mode as a direct footprint of re-hydrogenation.

Keywords:

## I. INTRODUCTION

Ever since its first isolation from graphite [1], graphene has captured great attention from the scientific community. Graphene is a 2D material of  $sp^2$ -coordinated carbon atoms arranged in a honeycomb lattice. The unique electrical, mechanical and thermal properties of this material make it attractive for numerous fields of application in science and technology [2, 3]. Moreover, the possibility to chemically functionalise the graphene lattice with hydrogen atoms is a further promising feature. When hydrogen atoms attach to the  $sp^2$ -coordinated carbon atoms of graphene, a distortion of the lattice toward an  $sp^3$  configuration leads to the transition from a zero-gap (graphene) to a wide-gap semiconductor (fully hydrogenated graphene) [4, 5]. Due to these unique properties of broad interest, the hydrogenation of graphene has been widely investigated in the last decades both in terms of graphene synthesis and structure and in terms of hydrogenation techniques [6–19].

In the context of sustainable and alternative source of energy, the use of hydrogen as a fuel is one of the most promising and studied possibilities. The common solutions for hydrogen storage are indeed the cryogenic liquid form or the compressed gas state, both presenting considerable disadvantages first of which a safety related issue [20, 21]. Along with metal hydrides, a valuable alternative is represented by carbon-based structures, which allow to have a safe, reversible, compact and high-loading - 1:1 proportion of H:C eventually - solid state form hydrogen storage [20–22].

Tritium is a radioactive hydrogen isotope that has the same chemical properties of its stable counterpart. Great interest in tritium handling lies in its use as a sustainable fuel for next-generation nuclear fusion energy reactors [23]. It follows that, as hydrogen can be stored in a solid state form chemically bonded to graphene, the analogous can be achieved with tritium [24]. Therefore, graphene can represent also a promising alternative for tritium storage to the most widely adopted uranium-alloys [23]. Furthermore, graphene plays a major role in the tritium handling chain as it can be employed for hydrogen isotopes separation via electrochemical pumping, thus exploiting the graphene selective permeation [25, 26].

The bonding of atomic tritium to graphene is also important in neutrino physics, for example in the PTOLEMY project [27–29]. This experiment aims to measure the neutrino mass with an unprecedented energy resolution and, eventually, unveil the cosmic neutrino background from the study of the endpoint of the  $\beta$ -spectrum of tritium. One of the

most important novelties introduced by the PTOLEMY experiment is a solid state target, with atomic tritium bonded to graphene nanostructures (*i.e.* nanoporous graphene, stacked monolayer graphene sheets or carbon nanotubes).

In all the above mentioned frameworks, both involving hydrogen and tritium, the stability of the functionalised graphene surface in different environments is a critical topic - especially to avoid ambient contamination with tritium. The dehydrogenation and degradation of hydrogenated graphene both in air and in different chemical (oxidant) environments, has been studied in a few works via Raman spectroscopy, infrared spectroscopy and resistance experiments [30–32]. However, a systematic investigation of the H-C chemical and bonding stability, also in view of the application to tritium, is still lacking. In this work, an extensive study on the stability of hydrogenated monolayer graphene in ultra-high vacuum and in air via X-ray photoemission spectroscopy (XPS) is reported. The recovery of the hydrogenated graphene after oxidation in air with atomic hydrogen exposure is also investigated via both XPS and electron energy loss spectroscopy (EELS). With the XPS technique, the C 1s core level spectrum is measured in order to study the evolution of the  $sp^2$  and  $sp^3$  coordinations of carbon atoms and the presence of carbon oxides. On the other hand, EELS measurements allow to observe the CH stretching mode as a direct footprint of the hydrogen bonding to carbon [33].

Finally, in the case of tritium bonded to graphene, one should take into account also the possible degradation of the surface due to the radioactivity of the isotope. Therefore, some considerations on the stability of tritiated graphene are discussed on the basis of the experimental experience with electron and ion bombardment of surfaces.

## II. SAMPLE PREPARATION AND EXPERIMENTAL METHODS

The samples investigated in this work are prepared at CNI@NEST laboratory in Pisa following the procedure thoroughly described in [34]. They consist in polycrystalline monolayer graphene grown via chemical vapor deposition (CVD) on electropolished copper [35, 36], then transferred onto a transmission electron microscopy (TEM) nickel grid (Ted Pella Inc. G2000HAN) with the standard wet etching technique [35, 37, 38]. After preparation, the samples are inserted in the ultra-high vacuum (UHV) chamber of the LASEC laboratory in Roma Tre University, where a 550 °C annealing is performed in order to clean the graphene

from PMMA (polymethyl methacrylate) residues due to the transfer procedure [34]. The hydrogenation is then carried out by exposing the samples to thermally-cracked atomic hydrogen (FOCUS EFM-H) while keeping the hydrogen partial pressure at  $3.6 \cdot 10^{-6}$  mbar. The hydrogenated samples herein investigated are the same described in [19], where a first sample (sample A) reached the hydrogen saturation level (59%  $sp^3$ ) after a dose of 320 kL, while the second one (sample B) after 260 kL (100%  $sp^3$ ).

The UHV chamber (base pressure  $10^{-9}$  mbar) is equipped with the experimental apparatuses for XPS and EELS. The XPS apparatus consists in an Omicron XM1000 monochromatised Al K $\alpha$  X-ray source ( $h\nu = 1486.7$  eV) and a hemispherical electron analyser (66 mm radius) with position sensitive detector for parallel acquisition. The total energy resolution for this technique is 460 meV and the binding energy scale has been calibrated by setting the C 1s core-level measured for clean highly oriented pyrolytic graphite (HOPG) at 284.5 eV [39]. The source of electrons for EELS is a custom-made monochromatic electron gun (45 meV energy resolution) operated at fixed electron energy of 91 eV [40], the electron analyser is the same used for XPS and the total energy resolution for EELS is 60 meV.

### III. EXPERIMENTAL RESULTS

#### In-vacuum and in-air stability of hydrogenated graphene

The effect of the hydrogen bonding to graphene is to distort the  $sp^2$  coordination of carbon atoms toward a  $sp^3$ -like configuration, with the hydrogen *pulling out* one carbon atom from the lattice plane [4, 5, 19]. Therefore, with XPS it is possible to study the C 1s core-level spectrum and use the  $sp^3$  contribution as a marker of graphene hydrogenation. In this perspective, the stability of hydrogen bonded to monolayer graphene was investigated by measuring the C 1s core-level time evolution: sample A was kept in the UHV chamber and measured after 4 months; sample B was taken out of the UHV chamber and remained in air (ambient atmospheric conditions) for 11 months before being measured again. In Figure 1(a), the C 1s spectra measured for sample A after hydrogen exposure and then after 4 months in UHV are shown. The C 1s line-shape resulted almost unchanged, suggesting a high stability of hydrogenated monolayer graphene in UHV for at least 4 months. On the other hand, a significant change in the spectrum was observed for sample B, which was kept

in air for 11 months after hydrogenation, as shown in Figure 1(b).

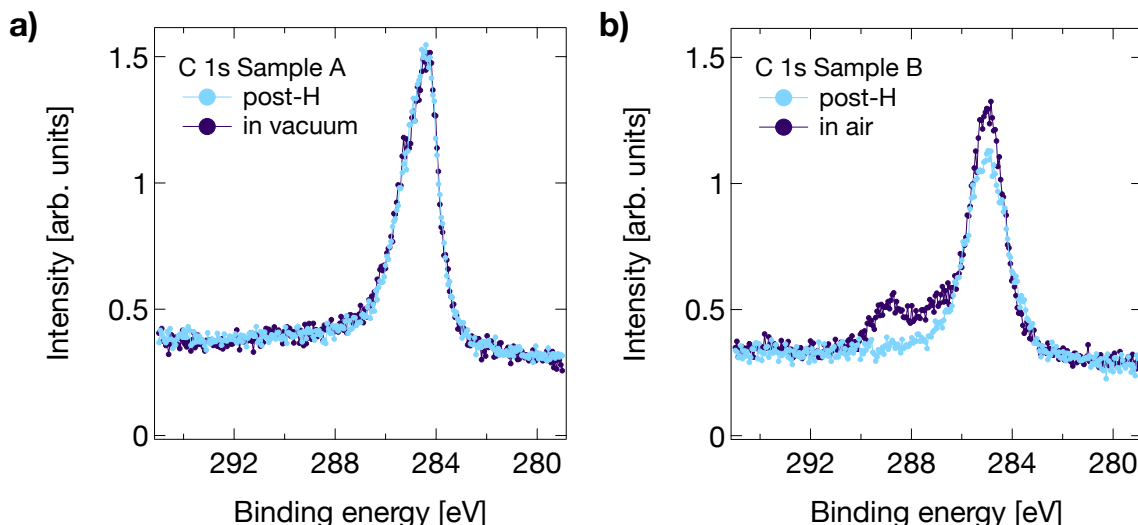


Figure 1: C 1s core-level spectra measured with XPS for: (a) sample A after hydrogenation (light blue) and after 4 months in UHV (purple); (b) sample B after hydrogenation (light blue) and after 11 months in air (purple).

A fit analysis has been carried out on the C 1s spectra in order to deconvolve the contributions of carbon atoms in different chemical configurations. For the analysis herein reported, a global fitting procedure has been employed (more details on this procedure can be found in [19, 41]). The analysis was carried out with a single global fit on all C 1s spectra presented in this work relative to both samples at each experimental step. In the  $sp^2$  component, all the Doniach-Sunjic line-shape parameters (asymmetry, Gaussian width and Lorentzian width) were free global parameters. All the other components ( $sp^3$ , C-O-C, O-C=O) were fitted with symmetric profiles, where the binding energy shifts, with respect to the  $sp^2$  position, and the Gaussian and Lorentzian widths were free global parameters. The area of the components in all the spectra were instead free individual parameters. Moreover, to perform this global fit analysis also the spectra acquired at each hydrogenation step were included (the results relative to the hydrogenation process can be found in [19]).

In Figure 2, the results of the global fit analysis for samples A and B, after exposure to hydrogen and after 4 months in vacuum and 11 in air respectively, are shown. For sample A,

which was kept in vacuum, the fit confirmed the high stability of the hydrogenated monolayer graphene. Indeed, the  $sp^3$  relative intensity, represented by the area ratio  $\frac{sp^3}{sp^2+sp^3}$ , varies by  $(4 \pm 2)\%$ . In the case of sample B, which reached an almost 100%  $sp^3$  saturation after hydrogen exposure, the 11 months in air led instead to a significant oxidation. The global fit revealed, indeed, the rise of two components that can be attributed to carbon bonded to oxygen in different configurations: the component at 286.8 eV associated to C-O-C and the component at 288.8 eV related to O-C=O [42–44]. Finally, the increase in the intensity of the  $sp^3$  component can be attributed to adsorbed carbon-based contaminants on the surface, non resolved in the spectrum.

As a confirmation of the hydrogen-induced oxidation of graphene, Figure 3 shows the C 1s spectrum of non-hydrogenated sample A before and after air-exposure. The measurement was carried out after 28 days in air and the carbon-oxygen component at 285.5 eV is only 8% of the C 1s total area. Therefore after air exposure, the non-hydrogenated sample shows a significantly lower oxygen contamination with respect to the hydrogenated ones.

### Re-hydrogenation of oxidised graphene

The *reversibility* of the oxidation process of hydrogenated graphene was studied on sample B. It was firstly annealed at 250 °C in vacuum in order to remove adsorbed contaminants and then exposed again to atomic hydrogen in two steps of 40 kL each. The effects on the C 1s line-shape can be observed in Figure 4(a) and in Figure 4(c) with the fit analysis.

The 250 °C annealing of the sample produced a significant reduction of the  $sp^3$  intensity, probably due to the desorption of contaminants from the surface, while it has no clear effects on the graphene oxidation (C-O-C and O-C=O components). The latter are, on the contrary, strongly affected by re-exposure of the sample to atomic hydrogen: significantly reduced after 40 kL and almost completely removed with 80 kL. The consequences of these treatments find confirmation in the behaviour of the O 1s core-level spectrum, shown in Figure 4(b). The annealing does not affect significantly the intensity of the spectrum, while it is drastically reduced after H-exposure. It is important to point out that the measured oxygen can come from both the graphene and the nickel of the TEM grid, bonded or adsorbed. However, the difference around 532.2 eV between the hydrogenated and re-hydrogenated (80 kL) O 1s spectra can be ascribed to residual C=O bondings [43]. This is also in agreement with the

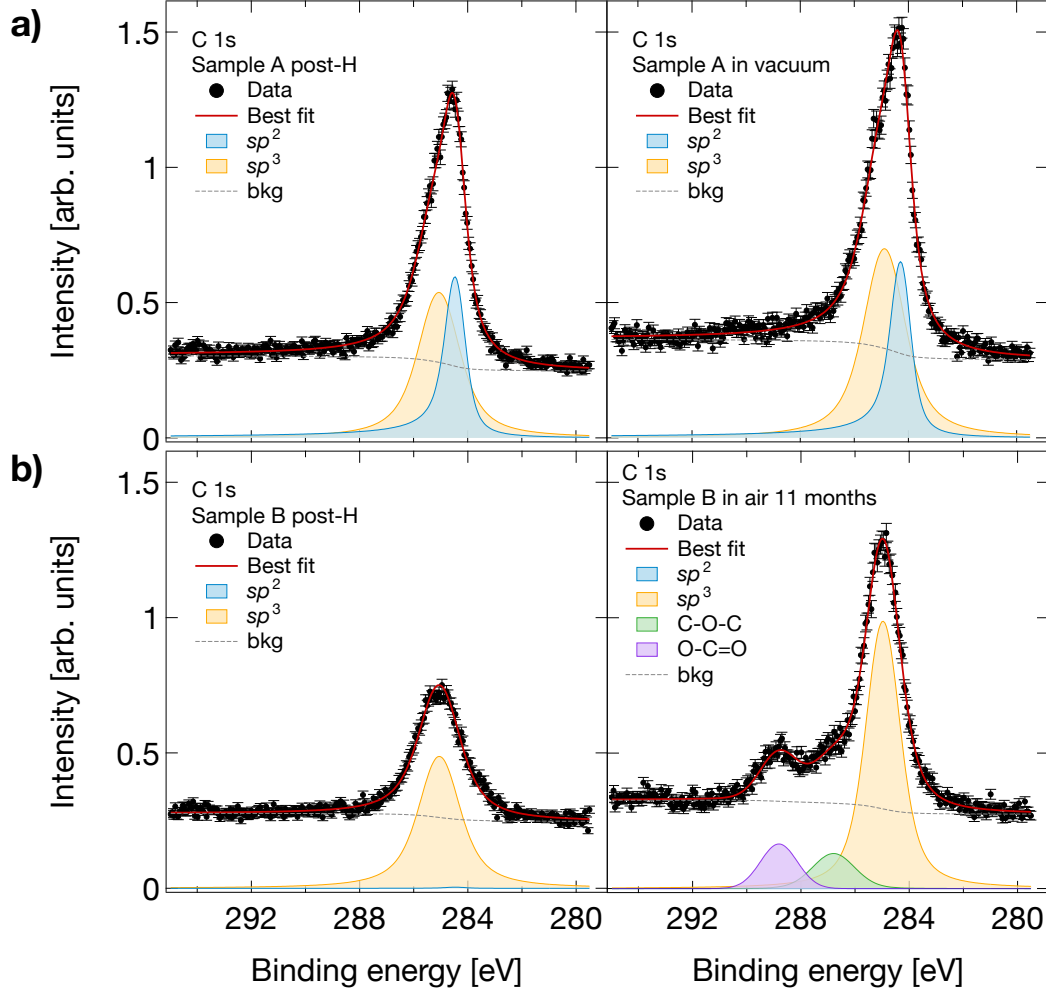


Figure 2: Fit analysis of the C 1s core-level spectra: (a) sample A after hydrogen exposure (left) and after 4 months in UHV (right); (b) sample B after hydrogen exposure (left) and after 11 months in air (right). The black dots represent the experimental data, the best fit curve is shown with red solid line, the shadowed curves are the  $sp^2$  (blue),  $sp^3$  (yellow), C-O-C (green) and O-C=O (violet) components and finally the dashed grey line is the integral background.

result of the C 1s fit analysis, in which the O-C=O component is almost but not completely removed.

After re-exposure to atomic hydrogen of sample B, the CH-stretching vibrational mode was measured with EELS as a further confirmation, and direct footprint, of re-hydrogenation



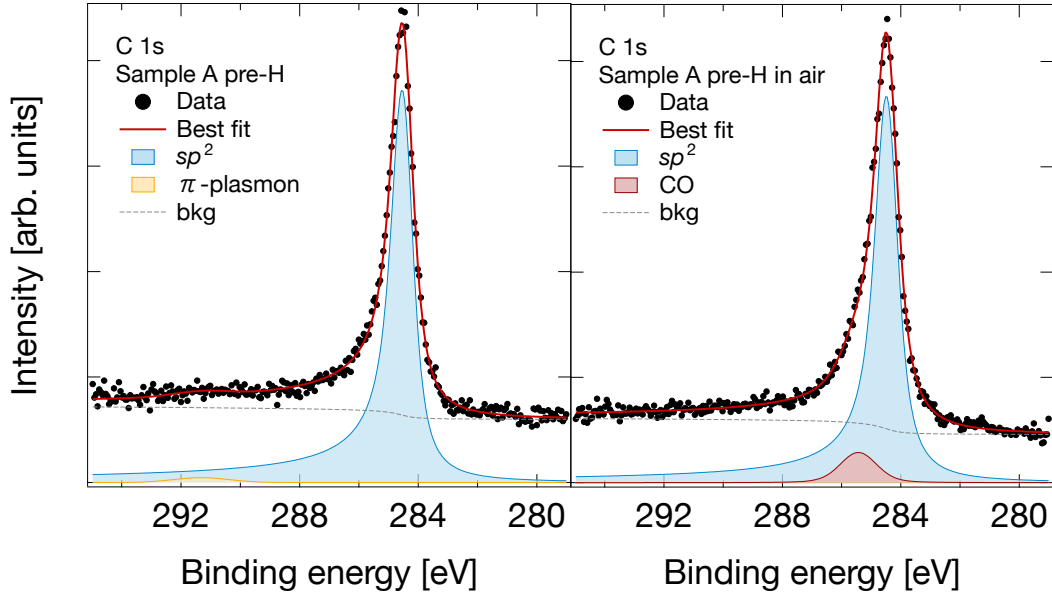


Figure 3: C 1s core level spectrum of non-hydrogenated sample A before and after air-exposure, along with a fit analysis. Representation follows same criteria used in Figure 2 except for  $\pi$ -plasmon component shown in yellow and C-O-C component in red.

[33]. The spectra were acquired in the vibration region in order to study the evolution of the CH-stretch mode, before and after re-hydrogenation. The EELS spectra for sample B before hydrogen exposure, after first exposure and after re-exposure (80 kL) are shown in Figure 5. The CH-stretching is well visible at 350 meV after both hydrogenation and re-hydrogenation as a direct evidence of the hydrogen bonding to graphene (further details on the EELS spectrum of sample B after the first hydrogenation can be found in [19]).

### Oxidation time scale of air-exposed hydrogenated graphene

With the aim of studying the oxidation process time scale of hydrogenated graphene, the C 1s core-level was measured as a function of time in air. The experiment was performed on sample B after a 90 kL re-hydrogenation and by keeping the sample out of the UHV chamber for 0.5, 1.5, 5, 18.5, 80 hours (cumulative). At each step the C 1s core-level was measured and the spectra are reported in Figure 6(a), along with the fitting curves. The relative intensity of the carbon oxides (sum of C-O-C and O-C=O components over the total C 1s intensity) follow an exponential behaviour up to saturation as a function of the

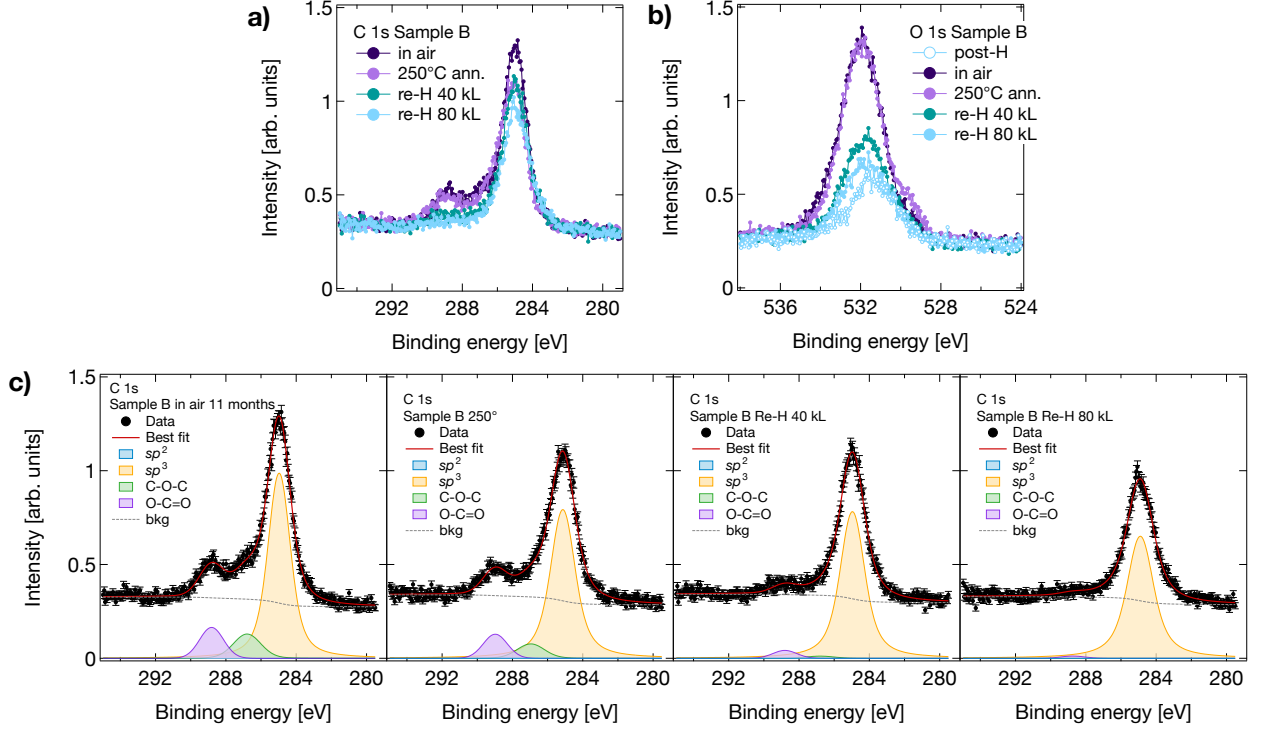


Figure 4: (a) C 1s and (b) O 1s core-level spectra of sample B measured after 11 months in air (purple), 250 °C annealing (violet), first (cyan) and second (light blue) step of re-hydrogenation. In (b) also the O 1s spectrum of sample B after hydrogenation is shown with empty dots. (c) Fit analysis of the C 1s core level for each step: 11 months in air, 250 °C annealing, first (40 kL) and second (80 kL) re-hydrogenation. Color coding follows same criteria used in Figure 2.

air-exposure time, as shown in Figure 6(b). Thus, the time-scale of the oxidation process for hydrogenated graphene has been evaluated through an exponential fit ( $a + be^{-x/\tau}$ ) of the carbon oxide relative intensity, resulting in a time constant  $\tau = 1.8 \pm 0.2$  hours.

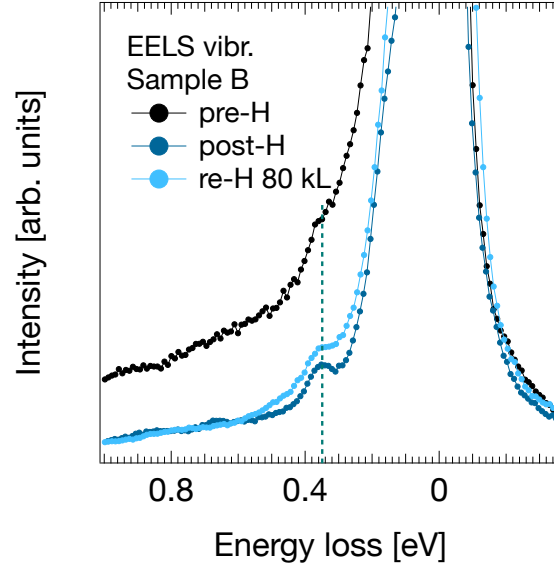


Figure 5: Vibrational EELS spectra measured on sample B before the hydrogenation (black), after the hydrogenation (blue) and after the re-hydrogenation (light blue). The dashed line guides the eye to the peak associated to the CH-stretching at 350 meV.

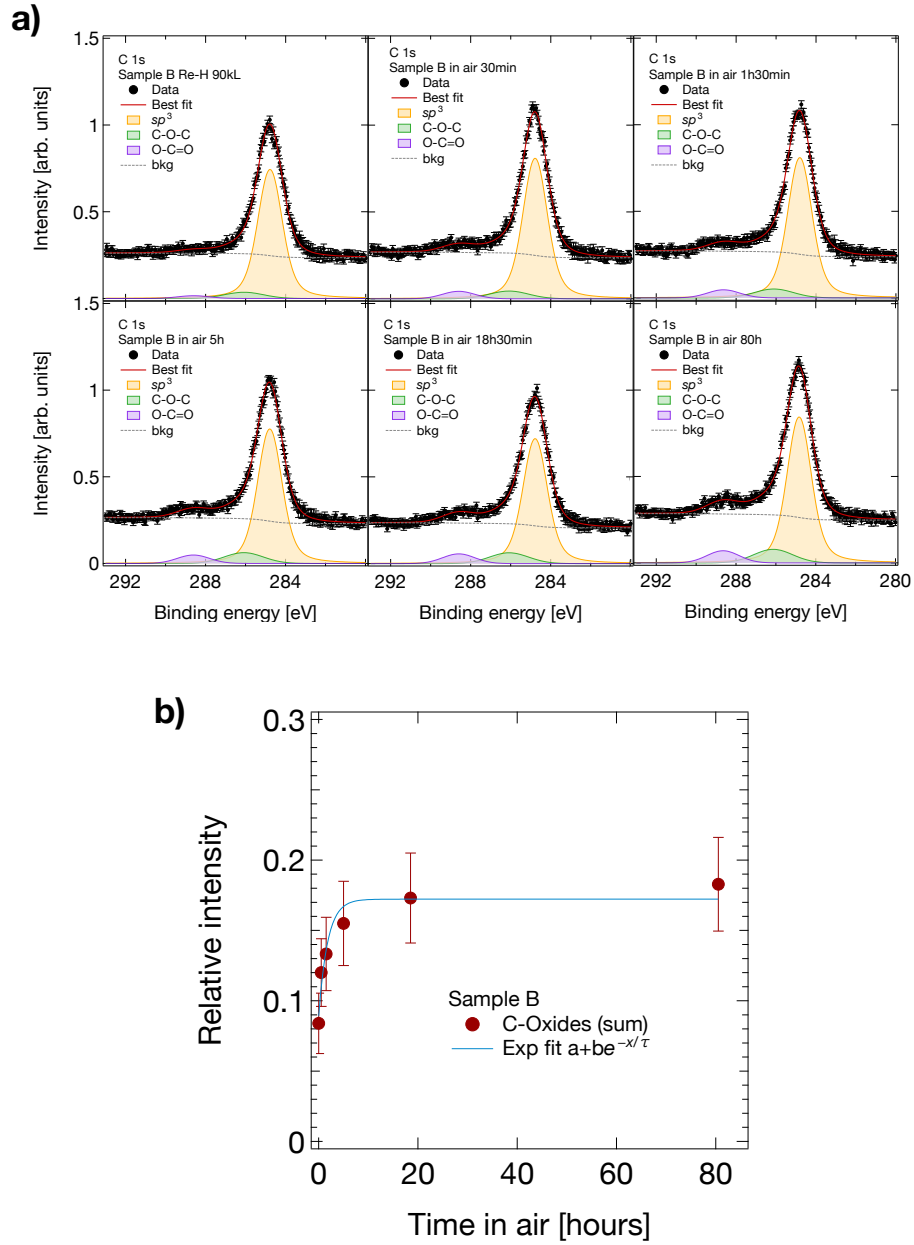


Figure 6: (a) C 1s spectra, with fit analysis, measured on sample B after a 90 kL re-hydrogenation and after 0.5, 1.5, 5, 18.5, 80 hours of (cumulative) air exposure. Curve representation follows same criteria used in Figure 2. (b) Sum of C-O-C and O-C=O intensities over the total C 1s intensity (red dots) versus air-exposure time of sample B, with exponential fit (blue line). First point at time 0 hours refers to re-hydrogenated sample.

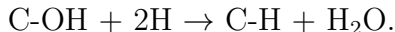
## IV. DISCUSSION

### Stability of hydrogenated graphene and re-hydrogenation

The herein reported results have shown the long-term stability - over 4 months - of hydrogenated graphene in ultra-high vacuum, as opposed to its high reactivity in atmospheric conditions. However, despite the significant oxidation in air, it has also been observed that it is possible to recover hydrogenated graphene after re-exposure to atomic hydrogen. The latter process is far from surprising, as irradiation with atomic hydrogen is, among others, a known method for the reduction of graphene oxide [45, 46]. Atomic hydrogen can indeed react on the graphene surface and remove oxygen, through the formation of hydroxyl radicals OH. Depending on the carbon-oxygen bonding, three different processes can occur on the surface [45, 46]:

1.  $\text{C-O-C} + 2\text{H} \rightarrow \text{C-OH} + \text{C-H}$ ;
2.  $\text{C=O} + 2\text{H} \rightarrow \text{H-C-OH}$ ;
3.  $\text{O=C-OH} + \text{H} \rightarrow \text{HO-C-OH}$ .

Under further reaction of OH radicals with H atoms, hydrogenated graphene can be restored as follows:



On the other hand, the oxidation process of hydrogenated graphene in atmospheric conditions is still not clear. There are a few available studies on the stability of hydrogenated graphene in air and the oxidation and dehydrogenation is also observed [31, 32]. In particular, the results reported in [31] show a different reactivity of hydrogenated graphene depending on the substrate. The dehydrogenation is experimentally investigated via Raman spectroscopy in [31] and Fourier transform infrared spectroscopy in [32]. The results, including the ones reported in this work, seem to have a non-good agreement with each other and to point out different outcomes for the exposure of hydrogenated graphene to air. Indeed, a dehydrogenation and recovery of graphene is claimed in [31], while signs of oxidation and dehydrogenation are shown in [32]. Furthermore, also the reported time-scales of the processes are different, hours in our case and days in [31]. In this regard, it should be

considered that the specific substrate on which the hydrogenated graphene is deposited can strongly affect its reactivity, as extensively discussed in [31]. Finally, due to the essentially uncontrolled nature of surface reactions occurring with air in atmospheric conditions, the dehydrogenation and oxidation processes of hydrogenated graphene are intrinsically hard to be well understood.

### Considerations on the tritium storage with graphene

In the context of using graphene as a solid-state reservoir for atomic tritium, in a neutrino physics experiment - such as PTOLEMY [27–29] - as well as in fusion energy experiments [23], the results reported in this work provide a clear indication: tritiated (hydrogenated) graphene should be kept in vacuum to preserve the surface functionalisation and, no less important, to avoid the release of tritium in air. However, while for hydrogenated graphene the in-vacuum condition is the only concern for the surface stability, in the case of tritiated graphene the  $\beta$ -decay could contribute to sample degradation as well. In particular, the emitted  $\beta$ -electrons and the recoiling  $^3\text{He}^+$  ions may damage the graphene lattice (*radiolysis*). In this regard, some rough considerations can be done to evaluate the relevance of the radiolysis issue.

Let us firstly focus on the  $\beta$ -electrons. From theoretical calculations on the  $\beta$ -spectrum for tritium bonded to single-layer graphene [47], the rate of emitted electrons as a function of their kinetic energy can be obtained. If two possible scenarios for the final state -  $^3\text{He}^+$  bonded to graphene in the ground state and a free  $^3\text{He}^+$  - are considered, the rate of emitted electrons for 1  $\mu\text{g}$  of tritium results in a distribution with mean energy of 5.9 keV and end-point at 18.58 keV. The electrons that can cause damage to the surface are the ones with low energy ( $\leq 1$  keV) [34]. The electron current in this energy region is in the order of a few fA/eV, thus the integral of the current up to 1 keV will be of a few pA. This current is a factor 100 lower than the typical values we use for EELS measurements, such as the ones reported in the previous section, in which the sample is irradiated for more than 6 hours and no sign of sample damage has been ever observed. Furthermore, the electron beam employed for spectroscopy is focused on a small portion of the sample ( $\sim 0.5 \text{ mm}^2$ ), while for 1  $\mu\text{g}$  of tritium the  $\beta$ -electrons would be spread on the whole surface of  $\sim 10^3$  fully tritiated samples and emitted over the full solid angle ( $4\pi$ ). Therefore, from the comparison with

EELS measurements, in which the current density is at least a factor  $10^6$  higher, we expect the  $\beta$ -electrons to be harmless for the graphene surface.

On the other hand, the  $^3\text{He}^+$  ions recoil with kinetic energies of a few eV for each  $\beta$ -electron emitted up to end-point. Thus, the ion current is at most a few tens of pA and it is spread on the whole surface of  $\sim 10^3$  fully tritiated samples and over the full solid angle. An extreme opposite case can be considered for comparison: ion sputtering. Sputtering treatments are usually carried out in solid-state physics experiments to clean surfaces. Damages are intentionally induced by ripping atoms from the sample surface, typically bombarding it with an Ar ion beam for several minutes. The current density is in the order of 100 nA/mm<sup>2</sup>, the energy of the order of 1 keV. Therefore, even neglecting the ion energy  $10^3$  times lower, the current density for the  $^3\text{He}^+$  ions in the  $\beta$ -decay is at least a factor  $10^8$  lower with respect to the typical values used for sputtering.

To conclude, the comparison with EELS and Ar sputtering, one harmless and the second damaging but at least a factor  $10^8$  more intense, allow us to speculatively infer that radiolysis may not represent a critical issue for tritiated graphene. However, specific experiments will have to be carried out to confirm this argument.

## V. CONCLUSIONS

The experimental results reported in this work show a long-term stability of hydrogenated graphene in vacuum and the oxidation of the surface when exposed to atmospheric conditions. The study has been carried out with XPS measurements of the C 1s and O 1s core levels. The hydrogenated graphene sample that was kept in UHV shows a stability of the C 1s spectrum of  $(4 \pm 2)\%$  after 4 months. On the other hand, a significant oxidation of the sample exposed to air was observed. In order to determine the time-scale of the in-air oxidation process, a specific experiment was carried out by monitoring the C 1s spectrum of the sample as a function of the air exposure. The carbon oxides relative intensity shows a rapid growth up to saturation with a time constant  $\tau = 1.8 \pm 0.2$  hours. Finally, an effective method for the recovery of hydrogenated graphene after oxidation was found to be the re-exposure of the sample to atomic hydrogen.

The sample degradation when exposed to atmospheric conditions was found to result in the partial dehydrogenation and oxidation of the graphene. The comparison with other

experimental results available in literature is not straightforward, due to the complexity of the surface interaction with air, an essentially uncontrolled gas. However, the presented results, together with the previous ones, on the instability of hydrogenated graphene in air open the way to further investigations and eventually understandings.

In conclusion, graphene is a good candidate for hydrogen (or tritium) storage as long as it is kept in vacuum, to prevent dehydrogenation. In the case of tritiated graphene, rough considerations on the radiolysis have been pointed out on the basis of experimental experience with electron and ion bombardment of the surfaces. The radiolysis seems to do not represent a critical issue for tritiated graphene, although experimental confirmations of this hypothesis will be required further on.

### Acknowledgements

We are grateful to Gianfranco Paruzza of the INFN Roma Tre Mechanical Workshop for his technical support. We gratefully acknowledge financial support from MUR PRIN 2020 'ANDROMeDa' project (Contract No. PRIN 2020Y2JMP5). This project has received funding from the European Union's Horizon 2020 research and innovation programme Graphene Flagship under grant agreement No. 881603. We are also grateful to INFN CSN5 for the financial support in this research.

- 
- [1] K. S. Novoselov, A. K. Geim, S. V. Morozov, D. Jiang, Y. Zhang, S. V. Dubonos, I. V. Grigorieva, and A. A. Firsov, *Science* **306**, 666 (2004), <https://www.science.org/doi/pdf/10.1126/science.1102896>, URL <https://www.science.org/doi/abs/10.1126/science.1102896>.
  - [2] K. S. Novoselov, A. K. Geim, S. V. Morozov, D. Jiang, M. I. Katsnelson, I. V. Grigorieva, S. V. Dubonos, and A. A. Firsov, *Nature* **438**, 197 (2005), ISSN 1476-4687.
  - [3] D. G. Papageorgiou, I. A. Kinloch, and R. J. Young, *Progress in Materials Science* **90**, 75 (2017), ISSN 0079-6425, URL <https://www.sciencedirect.com/science/article/pii/S0079642517300968>.
  - [4] D. W. Boukhvalov, M. I. Katsnelson, and A. I. Lichtenstein, *Physical Review B* **77**, 035427



- (2008), ISSN 1098-0121, 1550-235X.
- [5] J. O. Sofo, A. S. Chaudhari, and G. D. Barber, *Physical Review B* **75**, 153401 (2007), ISSN 1098-0121, 1550-235X.
  - [6] Z. Luo, J. Shang, S. Lim, D. Li, Q. Xiong, Z. Shen, J. Lin, and T. Yu, *Applied Physics Letters* **97**, 233111 (2010), ISSN 0003-6951, 1077-3118.
  - [7] J. S. Burgess, B. R. Matis, J. T. Robinson, F. A. Bulat, F. Keith Perkins, B. H. Houston, and J. W. Baldwin, *Carbon* **49**, 4420 (2011), ISSN 00086223.
  - [8] F. Zhao, Y. Raitses, X. Yang, A. Tan, and C. G. Tully, *Carbon* **177**, 244 (2021), ISSN 00086223.
  - [9] D. C. Elias, R. R. Nair, T. M. G. Mohiuddin, S. V. Morozov, P. Blake, M. P. Halsall, A. C. Ferrari, D. W. Boukhvalov, M. I. Katsnelson, A. K. Geim, et al., *Science* **323**, 610 (2009), ISSN 0036-8075, 1095-9203.
  - [10] S. Ryu, M. Y. Han, J. Maultzsch, T. F. Heinz, P. Kim, M. L. Steigerwald, and L. E. Brus, *Nano Letters* **8**, 4597 (2008), ISSN 1530-6984, 1530-6992.
  - [11] Z. Luo, T. Yu, K.-j. Kim, Z. Ni, Y. You, S. Lim, Z. Shen, S. Wang, and J. Lin, *ACS Nano* **3**, 1781 (2009), ISSN 1936-0851, 1936-086X.
  - [12] A. Felten, D. McManus, C. Rice, L. Nittler, J.-J. Pireaux, and C. Casiraghi, *Applied Physics Letters* **105**, 183104 (2014), ISSN 0003-6951, 1077-3118.
  - [13] R. Balog, M. Andersen, B. Jørgensen, Z. Sljivancanin, B. Hammer, A. Baraldi, R. Larciprete, P. Hofmann, L. Hornekær, and S. Lizzit, *ACS Nano* **7**, 3823 (2013), ISSN 1936-0851, 1936-086X.
  - [14] M. Panahi, N. Solati, and S. Kaya, *Surface Science* **679**, 24 (2019), ISSN 00396028.
  - [15] A. Paris, N. Verbitskiy, A. Nefedov, Y. Wang, A. Fedorov, D. Haberer, M. Oehzelt, L. Petaccia, D. Usachov, D. Vyalikh, et al., *Advanced Functional Materials* **23**, 1628 (2013), ISSN 1616-301X, 1616-3028.
  - [16] D. Haberer, D. V. Vyalikh, S. Taioli, B. Dora, M. Farjam, J. Fink, D. Marchenko, T. Pichler, K. Ziegler, S. Simonucci, et al., *Nano Letters* **10**, 3360 (2010), ISSN 1530-6984, 1530-6992.
  - [17] M. M. S. Abdelnabi, E. Blundo, M. G. Betti, G. Cavoto, E. Placidi, A. Polimeni, A. Ruocco, K. Hu, Y. Ito, and C. Mariani, *Nanotechnology* **32**, 035707 (2021), ISSN 0957-4484, 1361-6528.
  - [18] M. G. Betti, E. Placidi, C. Izzo, E. Blundo, A. Polimeni, M. Sbroscia, J. Avila, P. Dudin, K. Hu, Y. Ito, et al., *Nano Letters* **22**, 2971 (2022), pMID:

- 35294200, <https://doi.org/10.1021/acs.nanolett.2c00162>, URL <https://doi.org/10.1021/acs.nanolett.2c00162>.
- [19] A. Apponi, O. Castellano, D. Paoloni, D. Convertino, N. Mishra, C. Coletti, C. Mariani, and A. Ruocco (2025), arXiv:2504.10238 [cond-mat], URL <http://arxiv.org/abs/2504.10238>.
  - [20] A. Dillon and M. Heben, Applied Physics A Materials Science & Processing **72**, 133?142 (2001), ISSN 0947-8396.
  - [21] K. Jastrzębski and P. Kula, Materials **14**, 2499 (2021), ISSN 1996-1944.
  - [22] O. K. Alekseeva, I. V. Pushkareva, A. S. Pushkarev, and V. N. Fateev, Nanotechnologies in Russia **15**, 273?300 (2020), ISSN 1995-0780, 1995-0799.
  - [23] M. Rethinasabapathy, S. M. Ghoreishian, S. Hwang, Y. Han, C. Roh, and Y. S. Huh, Advanced Materials **35**, 2301589 (2023), ISSN 0935-9648, 1521-4095.
  - [24] G. Zeller, D. Díaz Barrero, P. Wiesen, S. Niemes, N. Tuchscherer, M. Aker, A. M. W. Leonhardt, J. Demand, K. Valerius, B. Bornschein, et al., **6**, 2838?2849 (2024), ISSN 2516-0230.
  - [25] M. Lozada-Hidalgo, S. Zhang, S. Hu, A. Esfandiar, I. V. Grigorieva, and A. K. Geim, Nature Communications **8**, 15215 (2017), ISSN 2041-1723.
  - [26] S. Yasuda, H. Matsushima, K. Harada, R. Tanii, T.-o. Terasawa, M. Yano, H. Asaoka, J. S. Gueriba, W. A. Diño, and K. Fukutani, ACS Nano **16**, 14362 (2022), ISSN 1936-0851, 1936-086X.
  - [27] A. G. Cocco, G. Mangano, and M. Messina, Journal of Physics: Conference Series **110**, 082014 (2008), ISSN 1742-6596, URL <http://dx.doi.org/10.1088/1742-6596/110/8/082014>.
  - [28] M. G. Betti, M. Biasotti, A. Boscá, F. Calle, N. Canci, G. Cavoto, C. Chang, A. Cocco, A. Colijn, J. Conrad, et al., Journal of Cosmology and Astroparticle Physics **2019**, 047 (2019), URL <https://doi.org/10.1088/1475-7516/2019/07/047>.
  - [29] A. Apponi, M. Betti, M. Borghesi, N. Canci, G. Cavoto, C. Chang, W. Chung, A. Cocco, A. Colijn, N. D'Ámbrosio, et al., Journal of Instrumentation **17**, P05021 (2022), URL <https://doi.org/10.1088/1748-0221/17/05/p05021>.
  - [30] P. Kula, W. Szymanski, L. Kolodziejczyk, R. Atraszkiewicz, J. Grabarczyk, M. Clapa, L. Kaczmarek, A. Jedrzejczak, and P. Niedzielski, Vacuum **129**, 79?85 (2016), ISSN 0042-207X.
  - [31] K. E. Whitener, J. T. Robinson, and P. E. Sheehan, Langmuir **33**, 13749?13756 (2017), ISSN 0743-7463, 1520-5827.
  - [32] L. Kaczmarek, T. Warga, P. Zawadzki, M. Makowicz, B. Bucholc, and P. Kula, International

- Journal of Hydrogen Energy **44**, 23149?23159 (2019), ISSN 03603199.
- [33] G. Di Filippo, A. Liscio, and A. Ruocco, Applied Surface Science **512**, 145605 (2020), ISSN 0169-4332, URL <https://www.sciencedirect.com/science/article/pii/S0169433220303615>.
  - [34] A. Apponi, D. Convertino, N. Mishra, C. Coletti, M. Iodice, F. Frascioni, F. Pilo, N. S. Blaj, D. Paoloni, I. Rago, et al., Carbon **216**, 118502 (2024), ISSN 0008-6223, URL <https://www.sciencedirect.com/science/article/pii/S0008622323007479>.
  - [35] V. Miseikis, D. Convertino, N. Mishra, M. Gemmi, T. Mashoff, S. Heun, N. Haghighian, F. Bisio, M. Canepa, V. Piazza, et al., 2D Materials **2**, 014006 (2015), URL <https://doi.org/10.1088/2053-1583/2/1/014006>.
  - [36] D. Convertino, F. Fabbri, N. Mishra, M. Mainardi, V. Cappello, G. Testa, S. Capsoni, L. Albertazzi, S. Luin, L. Marchetti, et al., Nano Letters **20**, 3633 (2020), pMID: 32208704, <https://doi.org/10.1021/acs.nanolett.0c00571>, URL <https://doi.org/10.1021/acs.nanolett.0c00571>.
  - [37] X. Li, W. Cai, J. An, S. Kim, J. Nah, D. Yang, R. Piner, A. Velamakanni, I. Jung, E. Tutuc, et al., Science **324**, 1312 (2009), <https://www.science.org/doi/pdf/10.1126/science.1171245>, URL <https://www.science.org/doi/abs/10.1126/science.1171245>.
  - [38] A. J. Marsden, M. Skilbeck, M. Healey, H. R. Thomas, M. Walker, R. S. Edwards, N. A. Garcia, V. Filip, H. Jabraoui, T. R. Walsh, et al., Phys. Chem. Chem. Phys. **24**, 2318 (2022), URL <http://dx.doi.org/10.1039/D1CP04316A>.
  - [39] X. Chen, X. Wang, and D. Fang, Fullerenes, Nanotubes and Carbon Nanostructures **28**, 1048 (2020), <https://doi.org/10.1080/1536383X.2020.1794851>, URL <https://doi.org/10.1080/1536383X.2020.1794851>.
  - [40] A. Apponi, F. Pandolfi, I. Rago, G. Cavoto, C. Mariani, and A. Ruocco, Measurement Science and Technology **33**, 025102 (2021), URL <https://doi.org/10.1088/1361-6501/ac3d07>.
  - [41] D. Paoloni and A. Ruocco, Surface Science **735**, 122322 (2023), ISSN 0039-6028, URL <https://www.sciencedirect.com/science/article/pii/S0039602823000754>.
  - [42] A. Kovtun, D. Jones, S. Dell’Elce, E. Treossi, A. Liscio, and V. Palermo, Carbon **143**, 268 (2019), ISSN 0008-6223, URL <https://www.sciencedirect.com/science/article/pii/S0008622318310297>.
  - [43] L. Stobinski, B. Lesiak, A. Malolepszy, M. Mazurkiewicz, B. Mierzwa, J. Zemek, P. Jiricek,

- and I. Bieloshapka, *Journal of Electron Spectroscopy and Related Phenomena* **195**, 145 (2014), ISSN 0368-2048, URL <https://www.sciencedirect.com/science/article/pii/S0368204814001510>.
- [44] F. Perrozzi, S. Croce, E. Treossi, V. Palermo, S. Santucci, G. Fioravanti, and L. Ottaviano, *Carbon* **77**, 473 (2014), ISSN 0008-6223, URL <https://www.sciencedirect.com/science/article/pii/S0008622314004928>.
- [45] A. Heya and N. Matsuo, *Thin Solid Films* **625**, 93?99 (2017), ISSN 00406090.
- [46] A. Jelea, F. Marinelli, Y. Ferro, A. Allouche, and C. Brosset, *Carbon* **42**, 3189?3198 (2004), ISSN 00086223.
- [47] A. Casale, Master's thesis, Sapienza Università di Roma (2023).